On roots and charts of delay equations with complex coefficients

Dimitri Breda *

* *Dipartimento di Matematica e Informatica*
Università degli Studi di Udine
via delle Scienze 206 I-33100 Udine, Italy
dimitri.breda@uniud.it

Abstract: this work is devoted to the analytic study of the characteristic roots of scalar autonomous Delay Differential Equations (DDEs) with complex coefficients. The focus is placed on the robust analysis of the position of the roots in $\mathbb{C}$ with respect to the variation of the coefficients, with the final aim of obtaining suitable representations for the relevant stability boundaries and charts. The investigation benefits from a preliminary shift of the coefficients which reduces the number of free parameters allowing for useful graphical visualizations. The present research is motivated on the base of studying the stability of *systems* of DDEs.

Keywords: delay differential equations, characteristic roots, stability charts, robust analysis

1. INTRODUCTION

Consider the autonomous system of DDEs

$$x'(t) = Ax(t) + Bx(t-\tau) \tag{1}$$

with a single constant delay $\tau > 0$ and $A, B \in \mathbb{R}^{m\times m}$. The asymptotic stability of (1) switches as the associated rightmost characteristic root crosses the imaginary axis. Despite its simplicity and to the best of the author's knowledge, the study of the stability of (1) through the analysis of the *exact* position in $\mathbb{C}$ of its roots w.r.t. A and B is still an open problem and a subtle issue (Hale, 1977, p.109), which nevertheless gave the start to a wide range of numerical investigations (e.g. Breda et al. (2005); Butcher et al. (2004); Engelborghs and Roose (2002); Jarlebring (2008); Vyhlídal and Zítek (2006)). It is known that the question can be reduced to that of scalar DDEs as far as A and B are simultaneously reducible to Schur form (e.g. Jarlebring and Damm (2007)). Precisely, suppose that there exists a unitary matrix U such that $A = UT_AU^H$ and $B = UT_BU^H$ with both T_A and T_B upper triangular. Then the stability problem for (1) can be trivially decomposed to the study of the m equations

$$x'(t) = a_ix(t) + b_ix(t-\tau),\ i = 1,\dots,m, \tag{2}$$

where a_i's and b_i's are the diagonal entries of T_A and T_B, respectively.

At this point, two important facts are worthy noticing: (i.) the case of simultaneous Schur factorization is the most general one potentially allowing for a complete study of the roots (and stability) of (1) in terms of the coefficients A and B, in view of the above reduction; (ii.) the study of the characteristic roots of (2) w.r.t. its coefficients is completely known as long as $a_i, b_i \in \mathbb{R}$, e.g. (Hale, 1977, p.109), but, in general, the above reduction can lead to $a_i, b_i \in \mathbb{C}$, a case for which a total and clear knowledge is not yet available (see e.g. Maset (2000)). Therefore this study aims at developing a complete analysis of the characteristic roots of (2) with $a_i, b_i \in \mathbb{C}$, attempting also to produce useful representations for the relevant stability boundaries in some suitable parameters plane (as it is the wide- and well-known case of real coefficients). DDEs with complex coefficients not coming from a Schur factorization arise in Sipahi et al. (2006).

With this objective, and without loss of generality, we consider the autonomous DDE with one unit delay

$$x'(t) = a_0x(t) + b_0x(t-1). \tag{3}$$

where $a_0, b_0 \in \mathbb{C}$ and $b_0 \neq 0$. The characteristic equation associated to (3) reads

$$F_0(\lambda) = 0 \tag{4}$$

where $\mathbb{C} \ni \lambda \mapsto F_0(\lambda) := \lambda - a_0 - b_0e^{-\lambda}$ is the characteristic function whose zeros λ, the solutions of (4), are the characteristic roots. The study of these latter is not as easy as that of the correspondent real case. Consider only the fact that they depend on the four *real* parameters $a_{0,R} := \Re(a_0)$, $a_{0,I} := \Im(a_0)$, $b_{0,R} := \Re(b_0)$ and $b_{0,I} := \Im(b_0)$. We then perform a preliminary shift of the coefficients of (3) which reduces the number of effective parameters from four to two. The advantage of this reduction is twofold: (i.) stability charts are suitably representable together with stability boundaries and all imaginary root crossings (i.e. bifurcation curves, number of unstable roots, etc.); (ii.) characteristic roots can be obtained (in principle analytically) starting from intersections of curves for the simplified shifted equation and then shifting them back to the original problem. Both targets are achieved by standard algebraic techniques similar to those used for the real case.

As a final remark, let us observe that the requirement for A and B in (1) to be simultaneously reducible to Schur form is a rather strict one (Radjavi and Rosenthal (2000)). However, we conjecture, mainly based on a large number of experimental observations, that a similar decomposition to n (perturbed) scalar equations is performable in a much wider fashion, probably with a more involved relation

between the scalar coefficients and the original matrix ones. If this were to hold true, the analysis of (3) would represent the constitutive brick of the whole structure. The author wishes to stress that a co-authored survey paper about the topic of roots and charts for DDEs in its generality is in preparation (Bozzo et al. (2010)).

The paper is organized as follows. Section 2 presents the shifting strategy. Section 3 deals with real, imaginary and crossing roots, respectively, of the shifted equation. Section 4 analyzes two families of curves whose intersection contains all characteristic roots. Finally, roots and stability charts for the original equation are obtained in Section 5.

Remark 1. (on notation). Throughout the paper, we set for brevity $\pi_k := k\pi$ and $\pi'_k := (2k+1)\frac{\pi}{2}$, $k \in \mathbb{Z}$.

2. SPECTRAL SHIFTING

Let $z \in \mathbb{C}$ be $z := z_R + \mathrm{i}z_I$ with $z_R = \Re(z)$, $z_I = \Im(z)$. Let $\lambda = \alpha + \mathrm{i}\beta$ be a characteristic root of (3) and set μ by imposing

$$\lambda = \mu + z.$$

Then, by substituting into (4) we get that μ is a solution of $\overline{F}(\mu) = 0$ where $\mathbb{C} \ni \mu \mapsto \overline{F}(\mu) := \mu - \overline{a} - be^{-\mu}$ with $\overline{a} = a_0 - z$ and $b = b_0 e^{-z}$. If we write $b_0 = |b_0|e^{\mathrm{i}\angle b_0}$ with $|b_0| = \sqrt{b_{0,R}^2 + b_{0,I}^2}$ and $\angle b_0 = \arctan\frac{b_{0,I}}{b_{0,R}}$, then we can choose z in such a way that $b \in \mathbb{R}$. In particular, it turns out that the choice $z_I = \angle b_0$ leads to $b = |b_0|e^{-z_R} \in \mathbb{R}^+$ ($b = 0$ is excluded by having assumed $b_0 \neq 0$). We see moreover that z_R can still be freely chosen. Then, by assuming $z_R = a_{0,R}$ we get also $\overline{a} = \mathrm{i}(a_{0,I} - \angle b_0) \in \mathrm{i}\mathbb{R}$. Set then $a := -\mathrm{i}\overline{a} = a_{0,I} - \angle b_0 \in \mathbb{R}$. We may resume the use of the shift by $z \in \mathbb{C}$ in the following.

Proposition 2. λ is a characteristic root of (3) if and only if $\mu = \lambda - z$ is a characteristic root of

$$x'(t) = \mathrm{i}ax(t) + bx(t-1) \tag{5}$$

with $a = a_{0,I} - \angle b_0 \in \mathbb{R}$ and $b = |b_0|e^{-a_{0,R}} \in \mathbb{R}^+$ whenever $z = a_{0,R} + \mathrm{i}\angle b_0$.

Proof. The proof was given above. ■

The characteristic equation associated to (5) reads

$$F(\mu) = 0 \tag{6}$$

where $\mathbb{C} \ni \mu \mapsto F(\mu) := \mu - \mathrm{i}a - be^{-\mu}$ is the characteristic function. Let us denote $\mu = \gamma + \mathrm{i}\delta$, $\gamma, \delta \in \mathbb{R}$, the solutions of (6), i.e. the characteristic roots of (5). It is clear that, as long as $\gamma, \delta \in \mathbb{R}$, if $\mu = \gamma + \mathrm{i}\delta$ is a characteristic root, then its conjugate $\overline{\mu} = \gamma - \mathrm{i}\delta$ is not a root anymore, rather it is a characteristic root of $x'(t) = -\mathrm{i}ax(t) + bx(t-1)$. Therefore, we assume without loss of generality that $\delta \geq 0$ and study only the case $a \in [0, +\infty)$.

By substituting in (6) we get the couple of real algebraic equations

$$\begin{cases} \gamma = be^{-\gamma}\cos\delta \\ a - \delta = be^{-\gamma}\sin\delta. \end{cases} \tag{7}$$

By squaring and adding member to member on the one hand and by taking their ratio (and excluding the cases $\delta = a$ and $\delta = \pi'_k$) on the other we get the system

$$\begin{cases} \gamma^2 + (a-\delta)^2 = b^2 e^{-2\gamma} \\ \dfrac{\delta - a}{\gamma} = -\tan\delta \end{cases} \tag{8}$$

which has, in $\mathbb{C} \setminus \{\mathbb{R} + \mathrm{i}a\}$, exactly double the solutions of (7). In fact, half of them are exactly the characteristic roots of (5), the others are the characteristic roots of

$$x'(t) = \mathrm{i}ax(t) - bx(t-1). \tag{9}$$

We now proceed to the analysis of the characteristic roots of (5) by discussing the solutions of (8), keeping in mind that we shall eventually eliminate those solutions corresponding to characteristic roots of (9).

Remark 3. The case $\delta = a$ can lead to a solution of (7) if and only if $\delta = \pi_k$, being $b \neq 0$. This is possible if and only if $a = \pi_k$, i.e. in a set of measure zero on the parameters plane (a, b).

The two following basic results hold trivially. They individuate a couple of curves in $\mathbb{C}$ whose intersection contain all the (infinitely-many, Hale (1977)) characteristic roots. These curves will be detailed in Section 4.

Proposition 4. If $\mu = \gamma + \mathrm{i}\delta$ is a characteristic root of (5), then (γ, δ) belongs to the graph of the curve

$$\mathbb{R} \ni \gamma \mapsto \mathcal{E}(\gamma) := a \pm \sqrt{b^2 e^{-2\gamma} - \gamma^2} \tag{10}$$

whenever the righthand side is well-defined.

Proof. Trivial from the first in (8). ■

Proposition 5. If $\mu = \gamma + \mathrm{i}\delta$ is a characteristic root of (5), then (γ, δ) belongs to the graph of the curve

$$\mathbb{R} \ni \delta \mapsto \mathcal{T}(\delta) := -\frac{\delta - a}{\tan\delta} \tag{11}$$

whenever the righthand side is well-defined.

Proof. Trivial from the second in (8). ■

In the sequel we shall again discuss separately the particular cases of pure real ($\delta = 0$) and imaginary ($\gamma = 0$) roots. This will be done with no reference to the above curves $\mathcal{E}$ and $\mathcal{T}$. Then, we shall address the analysis of the general properties of these latter, recovering also the results on the previous particular cases.

3. REAL, IMAGINARY AND UNSTABLE ROOTS

Let us assume $\delta = 0$ and hence $\mu = \gamma \in \mathbb{R}$. System (7) reduces to the single equation

$$\gamma = be^{-\gamma}, \tag{12}$$

being the second equation identically satisfied if and only if $a = 0$. This soon leads to the following.

Proposition 6. The trivial root $\mu = 0$ never exists.

Proof. Straightforward from (12). ■

In general, all possible solutions of (12) belong to the set of intersections of the line $l(\gamma) := \gamma$ with the exponential curve $e(\gamma) := be^{-\gamma}$. Based on this observation and on the fact that $b \in \mathbb{R}^+$, we prove the following.

Proposition 7. There exists always a unique real and positive characteristic root $\mu = \gamma$ of (5) if and only if $a = 0$. Moreover, μ is increasing with b and $\mu \to 0$ as $b \to 0$.

Proof. The proof follows from $l(\gamma) = e(\gamma)$. ■

Let us assume now $\gamma = 0$ and hence $\mu = \mathrm{i}\delta \in \mathrm{i}\mathbb{R}$. System (7) reduces to

$$\begin{cases} -b\cos\delta = 0 \\ \delta - a + b\sin\delta = 0, \end{cases} \tag{13}$$

by which an alternative proof of Proposition 6 is evident.

Since $b \neq 0$, it must be $\delta = \pi'_k$. By substituting into the second equation in (13) it follows $b = (-1)^k [a - \pi'_k]$. This leads to the following.

Proposition 8. If, for some $k \in \mathbb{Z}$, (a, b) belongs to the graph of the curve

$$[0, +\infty) \ni a \mapsto \mathcal{I}_k(a) := (-1)^k [a - \pi'_k], \qquad (14)$$

then $\mu = \mathrm{i}\pi'_k$ is a characteristic root of (5) and vice-versa.

Proof. Trivial from system (13). ■

The curve (14) consists of infinitely-many lines as depicted in Figure 1, each of which is characterized by one $k \in \mathbb{Z}$. Moreover, $\mathcal{I}_k$ has slope $+1$ if k is even and -1 if k is odd.

Remark 9. The (excluded but limiting) case $b = 0$ leads to a pure imaginary root $\mu = \mathrm{i}a$ for every choice of $a \in \mathbb{R}$, as it is easy to verify from (13).

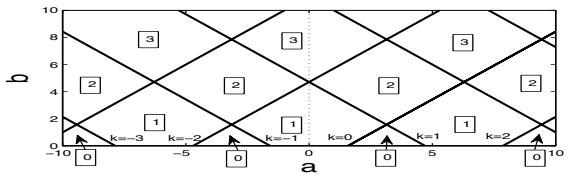

Figure 1. Imaginary crossings (14) in the parameters plane (a, b) and relevant numbers of unstable roots.

By combining the above results we are now able to locate all the curves in the parameters plane (a, b) along which crossings of the imaginary axis occur for the corresponding characteristic roots of (5), and we know that these occur only with $\delta \neq 0$. In particular the following result holds.

Proposition 10. A characteristic root μ of (5) crosses the imaginary axis if and only if (a, b) belongs to the graph of $\mathcal{I}_k$ in (14) for some $k \in \mathbb{Z}$. For that k, $\mu = \mathrm{i}\pi'_k$.

Proof. It is just an alternative formulation of Proposition 8. ■

Again, since the characteristic roots of DDEs are infinitely-many, but only a finite number of them is contained in any right-half of $\mathbb{C}$ (Hale, 1977, Section 1, Lemma 4.1), knowing the number of roots with positive real part for a given choice of (a, b) is enough to determine the same quantity in all the parameters plane through the foregoing results. This is justified by the fact that the roots depend continuously on the parameters.

We start with an easy choice, e.g. $(a, b) = (\pi, 1)$. Then (7) reads

$$\begin{cases} \gamma - e^{-\gamma} \cos \delta = 0 \\ \delta - \pi + e^{-\gamma} \sin \delta = 0. \end{cases}$$

From the second equation, by denoting $\epsilon = \pi - \delta$, we have

$$e^{\gamma} = \frac{|\sin \delta|}{|\pi - \delta|} = \frac{|\sin(\pi - \epsilon)|}{|\epsilon|} = \frac{|\sin \epsilon|}{|\epsilon|} \leq 1$$

and hence $\gamma < 0$, i.e. there cannot be *unstable* roots (i.e. with nonnegative real part). The case $\delta = \pi$ leads to $\gamma < 0$ anyway.

Now we study the direction of the crossings by a perturbation argument. Fix $k \in \mathbb{Z}$, k even, and choose a point (a, b) such that $b = \mathcal{I}_k(a)$. Then, for the choice $\delta_k = \pi'_k$, the root $\mu = \mathrm{i}\delta_k$ exists thanks to Proposition 8. Consider now $\varepsilon_a > 0$ sufficiently small, the perturbed point $(a + \varepsilon_a, b)$ and the corresponding perturbed root $\mu = \varepsilon_\gamma + \mathrm{i}(\delta_k + \varepsilon_\delta)$. The original point (a, b) satisfies

$$\begin{cases} -b \cos \delta_k = 0 \\ \delta_k - a + b \sin \delta_k = 0 \end{cases} \qquad (15)$$

while the perturbed one satisfies

$$\begin{cases} \varepsilon_\gamma - be^{-\varepsilon_\gamma} \cos(\delta_k + \varepsilon_\delta) = 0 \\ \delta_k + \varepsilon_\delta - (a + \varepsilon_a) + be^{-\varepsilon_\gamma} \sin(\delta_k + \varepsilon_\delta) = 0. \end{cases} \qquad (16)$$

By using (15), the sine and cosine sum laws and by observing that $\cos \delta_k = 0$ and $\sin \delta_k = 1$, (16) reduces to

$$\begin{cases} \varepsilon_\gamma = -be^{-\varepsilon_\gamma} \sin \varepsilon_\delta \\ \varepsilon_\delta = \varepsilon_a + b(1 - e^{-\varepsilon_\gamma} \cos \varepsilon_\delta). \end{cases} \qquad (17)$$

From the first one we get $\mathrm{sign}(\varepsilon_\gamma) = -\mathrm{sign}(b)\mathrm{sign}(\varepsilon_\delta)$ and, being $b > 0$, $\mathrm{sign}(\varepsilon_\gamma) = -\mathrm{sign}(\varepsilon_\delta)$. Suppose now, by contradiction, that $\varepsilon_\gamma > 0$. Then, simultaneously we get $e^{-\varepsilon_\gamma} = 1^-$, $\cos \varepsilon_\delta = 1^-$ and, from the second in (17), $\varepsilon_\delta > 0$. Consequently, $\varepsilon_\gamma < 0$, contradicting the assumption. The following result resumes and extends what above.

Proposition 11. A point (a, b) crossing the graph of $\mathcal{I}_k$ in (14) for some $k \in \mathbb{Z}$ generates a characteristic root $\mu = \mathrm{i}\pi'_k$ crossing the imaginary axis from the right to the left if k is even and vice versa if k is odd.

Proof. The proof for k even was given above. The proof for k odd is similar. ■

Now, by recalling that the only possible real roots are positive (and correspond to points $(0, b)$ in the parameters plane), we conclude that all bifurcations are of Hopf type and that the number of unstable roots in $\mathbb{C} \setminus \mathbb{R}$ is distributed as depicted in Figure 1. From this simple analysis we conclude that the region of asymptotic stability is represented by the lower triangular portions in Figure 1 included between the lines $b = \mathcal{I}_k(a)$ and the horizontal axis $b = 0$ as detailed in the following.

Proposition 12. If $\mu = \gamma + \mathrm{i}\delta$ is a characteristic root of (5), then

$$\gamma \leq 0 \Leftrightarrow \begin{cases} 0 \leq b \leq a - \pi'_k \text{ for } a \in [\pi'_k, \pi_{k+1}] \\ 0 \leq b \leq \pi'_{k+1} - a \text{ for } a \in [\pi_{k+1}, \pi'_{k+1}] \end{cases}$$

for some $k \in \mathbb{Z}$, k even.

Proof. Argumented above. ■

We terminate this Section by observing that the asymptotic stability regions mentioned in Proposition 12 refers to the shifted equation (5) and not to the original one (3). We will go back to this point in Section 5.

4. THE CURVES $\mathcal{E}$ AND $\mathcal{T}$

We analyze now the curve $\mathcal{E}$ introduced in (10). Recall that if $\mu = \gamma + \mathrm{i}\delta$ is a characteristic root of (5), then $\delta = \mathcal{E}(\gamma)$ by Proposition 4. Such a curve behaves asymptotically as the exponential $\mathcal{E}(\gamma) \approx a \pm |b| e^{-\gamma}$ when $\gamma \to -\infty$. Opposite, when $\gamma \to +\infty$ the curve is not defined. Hence γ must be bounded above, as is already known and similarly to the real case. Since the curve is decreasing (with + sign), in order to explore the behavior around the maximum

values attainable for γ, we search for the values γ for which $\mathcal{E}(\gamma) = a$, hence the zeros of $\mathcal{E} - a$. These latter are characterized by the intersection of the curves $l(\gamma) := \gamma$ and $e(\gamma) := be^{-\gamma}$ as discussed in Section 3. Since $b > 0$, there is always a unique possible real solution $\gamma > 0$. Such a solution tends to 0 when $b \to +\infty$ whereas it tends to $+\infty$ when $b \to 0$. Moreover, there are also spurious roots due to the squaring with respect to the original problem. In fact, $b^2e^{-2\gamma} - \gamma^2 = 0 \Leftrightarrow l(\gamma) = \pm e(\gamma)$, but the equality with minus sign gives raise to solutions which have to be discharged. These latter can be 0, 1 double or 2 distinct, the discriminant being given by the tangent conditions $-e'(\gamma) = l'(\gamma)$ and $-e(\gamma) = l(\gamma)$ leading to $\gamma = -1$ and $b = e^{-1}$. Therefore, while there is always a true value $\gamma > 0$ such that $\mathcal{E}(\gamma) = a$, if $b > e^{-1}$ there is no spurious value γ such that $\mathcal{E}(\gamma) = a$; if $b = e^{-1}$ there is one double spurious value $\gamma = -1$ such that $\mathcal{E}(\gamma) = a$; if $b < e^{-1}$ there are two distinct spurious values $\gamma_1 < -1 < \gamma_2$ such that $\mathcal{E}(\gamma_{1,2}) = a$; and the situation is represented in Figure 2.

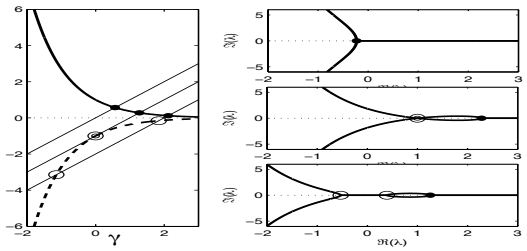

Figure 2. possible roots $\delta = a$ along $\mathcal{E}$ for $b > 0$. Left: intersections of $l(\gamma)$ with $\pm e(\gamma)$; right: curves $\mathcal{E}$ (top to bottom relevant to lines $l(\gamma)$ left to right), $\bullet$: true roots, $\circ$: spurious roots ($a = 0$ is represented).

We analyze now the curve $\mathcal{T}$ introduced in (11), Figure 3. Recall that if $\mu = \gamma + \mathrm{i}\delta$ is a characteristic root of (5), then $\gamma = \mathcal{E}(\delta)$ by Proposition 5. There is nothing particular to say about this curve except on how prolonging it by continuity. This can be done correspondingly to the values π'_k by setting $\mathcal{T}(\pi'_k) = 0$, in particular $\lim_{\delta \to \pi'^{\pm}_k} \mathcal{T}(\delta) = \mathrm{sign}(\pi'_k - a) \cdot (0^{\pm})$. Instead, correspondingly to the values π_k, there exist vertical asymptotes, in particular $\lim_{\delta \to \pi_k^{\pm}} \mathcal{T}(\delta) = \mathrm{sign}(\pi_k - a) \cdot (\mp\infty)$. Moreover, $\mathcal{T}'(\delta) = -\frac{1}{\sin^2 \delta}\left(\frac{1}{2}\sin 2\delta - \delta + a\right)$ and, consequently,

$$\mathrm{sign}(\mathcal{T}'(a)) = \begin{cases} -1 \text{ if } a \in (\pi_k, \pi'_k) \\ +1 \text{ if } a \in (\pi'_k, \pi_k)\,, \end{cases}$$

while

$$\mathrm{sign}(\mathcal{T}'(\pi'_k)) = \begin{cases} +1 \text{ if } \pi'_k > a \\ -1 \text{ if } \pi'_k < a. \end{cases}$$

Obviously, due to periodicity, the curve $\mathcal{T}$ is not invertible, but so is each of its branches, i.e. for $\delta \in [\pi_k, \pi_{k+1}]$.

We go back now to the relation between the characteristic roots of (5) and the intersection of the curves $\mathcal{E}$ and $\mathcal{T}$ as anticipated in Section 2. In particular, we focus on which half of the roots in $\mathbb{C} \setminus \{\mathbb{R} + \mathrm{i}a\}$ must be eliminated from $\mathcal{E} \cap \mathcal{T}$. Examples are given in Figure 4 for $a = 7$ and $b = 1$ and in Figure 5 for $a = -1$ and $b = 0.35$.

Proposition 13. $\mu = \gamma + \mathrm{i}\delta$ is a characteristic root of (5) if and only if $(\gamma, \delta) \in \mathcal{E} \cap \mathcal{T}$ and the signs of γ and $\delta - a$ match

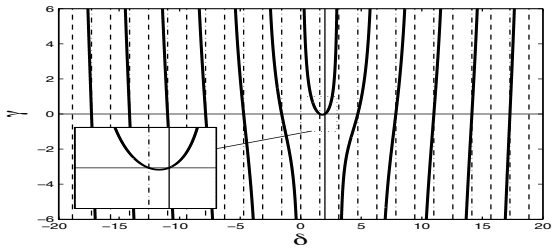

Figure 3. Curve $\mathcal{T}$ for $a = 2$ (solid-thick lines): dashed lines are the vertical asymptotes, dot-dashed lines are zeros, the solid horizontal line is $\gamma = 0$ and the vertical one is $\delta = a$.

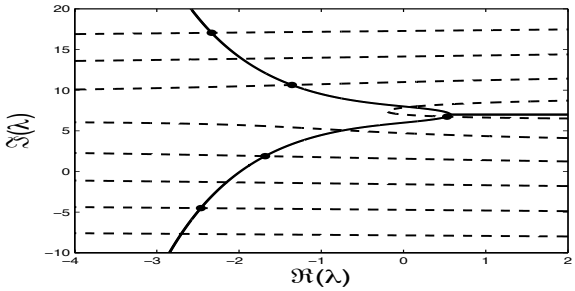

Figure 4. Roots of (5) ($\bullet$) and intersection of $\mathcal{E}$ (solid lines) and $\mathcal{T}$ (dashed lines) for $a = 7$ and $b = 1$.

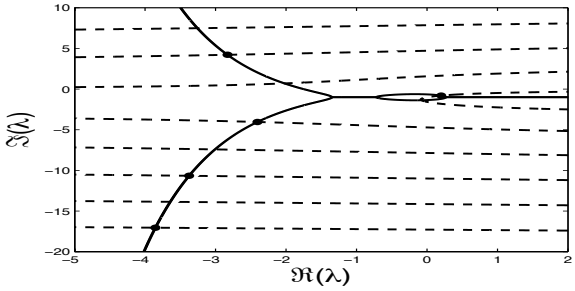

Figure 5. Roots of (5) ($\bullet$) and intersection of $\mathcal{E}$ (solid lines) and $\mathcal{T}$ (dashed lines) for $a = -1$ and $b = 0.35$.

the choices given in Table 1 (where k even is assumed without loss of generality).

Proof. The proof and the construction of the table of signs is based on (7) and on the fact that $b > 0$, hence: $\mathrm{sign}(\gamma) = \mathrm{sign}(\cos\delta)$ and $\mathrm{sign}(a - \delta) = \mathrm{sign}(\sin\delta)$. ■

	$[\pi_k, \pi'_k]$	$[\pi'_k, \pi_{k+1}]$	$[\pi_{k+1}, \pi'_{k+1}]$	$[\pi'_{k+1}, \pi_{k+2}]$
δ	$> a$	$> a$	$< a$	$< a$
γ	> 0	< 0	< 0	> 0
$\cos\delta$	> 0	< 0	< 0	> 0
$\sin\delta$	> 0	> 0	< 0	< 0

Table 1. Signs of γ and $\delta - a$ (k even).

Remark 14. In order to discharge those points in $\mathcal{E} \cap \mathcal{T}$ which are not characteristic roots of (5) it is enough to check one point with $\gamma < 0$ and $\delta > a$ (or $\delta \gg a$). Then, all the other roots are every second intersection from this one. This procedure avoids to start by checking which is the true root among the two intersections originated from the branch of $\mathcal{T}$ across $\delta = a$. This latter is, in fact, a little more involved.

5. BACK TO THE ORIGINAL EQUATION

We observed at the end of Section 3 that the regions of asymptotic stability individuated by Proposition 12 refer to the shifted DDE (5) with parameters $(a, b) \in \mathbb{R}\times\mathbb{R}^+$ and not to the original one (3) with parameters $(a_0, b_0) \in \mathbb{C}\times\mathbb{C}$.

By virtue of Proposition 2, we have that $\lambda = \alpha + \mathrm{i}\beta$ is a characteristic root of (3) if and only if

$$\lambda = (\gamma + a_{0,R}) + \mathrm{i}(\delta + \angle b_0), \tag{18}$$

where $\mu = \gamma + \mathrm{i}\delta$ is a characteristic root of (5). It is then obvious that the stability boundaries of the original DDE (3) are given by the curves in (a, b) generated by imposing $\gamma = -a_{0,R}$ (and not $\gamma = 0$ as it would be the case for the stability boundaries of the shifted DDE (5)). This final study will allow us to represent the stability boundaries of (3) in the two-dimensional parameters plane (a, b) instead that resorting to the larger four-dimensional parameters hyperplane $(a_{0,R}, a_{0,I}, b_{0,R}, b_{0,I})$, which makes no representation possible.

To perform such an analysis, let us consider (7) for $\gamma = -a_{0,R}$. From the first one we get $b = -\frac{a_{0,R}e^{-a_{0,R}}}{\cos\delta}$ and by substituting in the second one we get $a = \delta - a_{0,R}\tan\delta$ whenever $\delta \neq \pi'_k$. These latter individuate the curve $\mathbb{R} \ni \delta \mapsto \mathcal{D}(\delta) = (a(\delta), b(\delta))$ in (a, b) given by

$$\mathcal{D}(\delta) := \left(\delta - a_{0,R}\tan\delta, -\frac{a_{0,R}e^{-a_{0,R}}}{\cos\delta}\right). \tag{19}$$

We soon observe that $\delta = 0$ generates points on the vertical axis $a = 0$. But being $b > 0$, among such points only those satisfying $-a_{0,R}e^{-a_{0,R}} \geq e^{-1}$ are admissible (recall Section 3), i.e. when $a_{0,R} \leq e^{a_{0,R}-1}$. Observe now that it is not worthy to study (19) for all $\delta \in \mathbb{R}$, but it is enough to restrict to $\delta \in [0, \pi]$. In fact, being $\mathcal{D}(-\delta) = (-a(\delta), b(\delta))$ we know also what happens for $\delta \in [-\pi, 0]$. Then we can translate the obtained curve to the left (and to the right) by $2\pi_k$ for all $k \in \mathbb{Z}$ by virtue of the periodicity of $\tan\delta$ in $a(\delta)$ and of $\cos\delta$ in $b(\delta)$.

First of all, for $\delta \in [0, \pi]$, the curve (19) is not defined in $\delta = \frac{\pi}{2}$. Observe that $\lim_{\delta\to\frac{\pi}{2}^\pm} \mathcal{D}(\delta) = \mathrm{sign}(a_{0,R})\cdot(\pm\infty, \pm\infty)$, $\lim_{\delta\to\frac{\pi}{2}^\pm} \frac{b(\delta)}{a(\delta)} = e^{-a_{0,R}}$ and $\lim_{\delta\to\frac{\pi}{2}^\pm} [b(\delta) - e^{-a_{0,R}}a(\delta)] = 0$. Hence the line $b(a) = e^{-a_{0,R}}\left(a - \frac{\pi}{2}\right)$ is a oblique asymptote in the parameters plane (a, b). Moreover, we have $\mathcal{D}'(\delta) = \frac{b'(\delta)}{a'(\delta)} = \frac{-a_{0,R}e^{-a_{0,R}}\sin\delta}{\cos^2\delta - a_{0,R}}$ and hence, correspondingly to $\delta = 0$ and $\delta = \pi$ the curve has a horizontal tangent. Observe also that there is vertical tangency if $\delta = \arccos\sqrt{a_{0,R}}$, but this is the case only for $a_{0,R} \in (0, 1)$. The cases $a_{0,R} = 0$ and $a_{0,R} = 1$ are particular since coincident with $\delta = 0$ and $\delta = \pi$, respectively. Eventually we have $\mathcal{D}(0) = (0, -a_{0,R}e^{-a_{0,R}})$ and $\mathcal{D}(\pi) = (\pi, a_{0,R}e^{-a_{0,R}})$. The limiting condition to check whether these values are above or below the oblique asymptote is $a_{0,R} = \frac{\pi}{2}$.

In view of all what outlined above, we shall distinguish the cases (1) $a_{0,R} \in (-\infty, 0)$; (2) $a_{0,R} \in (0, 1)$; (3) $a_{0,R} \in \left(1, \frac{\pi}{2}\right)$ and (4) $a_{0,R} \in (1, +\infty)$ and focus on the values $a_{0,R} \in \left\{0, 1, \frac{\pi}{2}\right\}$ as particular and limiting ones. In Case (1), the curve $\mathcal{D}$ starts from $\mathcal{D}(0) = (0, -a_{0,R}e^{-a_{0,R}})$ and increases to the right towards the oblique asymptote as δ increases in $[0, \frac{\pi}{2})$, maintaining itself above this latter. Then it increases below the same asymptote as δ increases in $(\frac{\pi}{2}, \pi]$, reaching $\mathcal{D}(\pi) = (\pi, a_{0,R}e^{-a_{0,R}})$. This main branch is the solid curve in Figure 6. The other dashed ones are obtained by the symmetry reasonings discussed at the beginning. Being $b > 0$, only the first part is considered. In

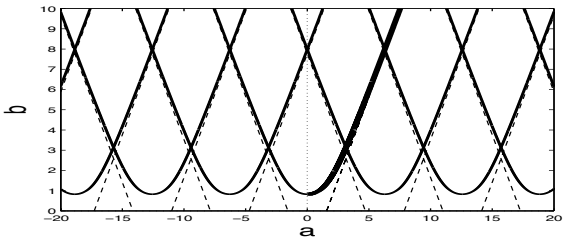

Figure 6. Imaginary crossings for $a_{0,R} = -0.5$: line for $\delta \in [0, \frac{\pi}{2})$ (solid thick) and oblique asymptotes (dashed).

Case (2), the principal branch for $\delta \in [0, \pi]$ is completely below the horizontal axis. Hence we describe the branch for $\delta \in [\pi, \frac{3\pi}{2})$, which is the right thick solid curve in Figure 7 (the left one is obtained by symmetry and corresponds to $\delta \in (-\frac{3\pi}{2}, -\pi]$). This branch starts horizontally from $\mathcal{D}(\pi) = (\pi, a_{0,R}e^{-a_{0,R}})$, increasing to the left, turning vertically and then backwards to the right, always below the oblique asymptote towards it. In Case (3), again the

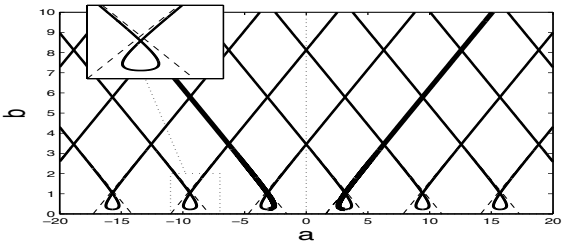

Figure 7. Imaginary crossings for $a_{0,R} = 0.3$: lines for $\delta \in [\pi, \frac{3\pi}{2})$ -right- and $\delta \in (-\frac{3\pi}{2}, -\pi]$ -left- (solid thick) and oblique asymptotes (dashed).

principal branch for $\delta \in [0, \pi]$ is completely below the horizontal axis. Hence we describe the secondary branch as in Case (1). This branch starts always horizontally from $\mathcal{D}(\pi) = (\pi, a_{0,R}e^{-a_{0,R}})$ (see the zoom in the top-right square), increasing directly to the right, always below the oblique asymptote and towards it. In Case (4), we

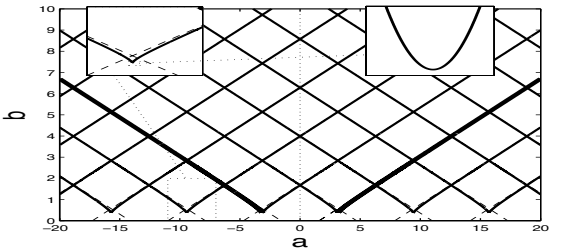

Figure 8. Imaginary crossings for $a_{0,R} = 1.01$: lines for $\delta \in [\pi, \frac{3\pi}{2})$ -right- and $\delta \in (-\frac{3\pi}{2}, -\pi]$ -left- (solid thick) and oblique asymptotes (dashed).

describe the secondary branch as in the previous Cases (2) and (3). This branch starts always horizontally from

$\mathcal{D}(\pi) = (\pi, a_{0,R}e^{-a_{0,R}})$, increasing to the right, this time above the oblique asymptote and towards it.

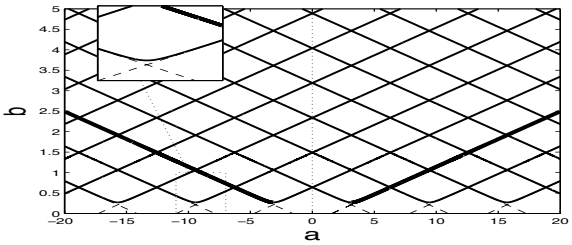

Figure 9. Imaginary crossings for $a_{0,R} = 2$: lines for $\delta \in [\pi, \frac{3\pi}{2})$ -right- and $\delta \in (-\frac{3\pi}{2}, -\pi]$ -left- (solid thick) and oblique asymptotes (dashed).

We complete the analysis by showing the configuration for the particular cases $a_{0,R} = 0$ in Figure 1 (in fact, whenever $a_{0,R} = 0$, the asymptotic stability regions of (5) and of (3) are the same), $a_{0,R} = 1$ in Figure 10 and $a_{0,R} = \frac{\pi}{2}$ in Figure 11. Starting from Figure 1, by a continuity argument, it is not difficult to argue that the same numbers of unstable roots can be distributed seemingly in the plots of all the other Figures 6, 7, 8, 9, 10 and 11. Among the many conclusions that can be driven, the following one results rather important.

Proposition 15. If $a_{0,R} \geq 1$, the region of asymptotic stability of (3) is empty.

Proof. Argumented above. ■

As far as $a_{0,R} = 1$, the zoom in the top square of Figure 10 shows that this is the only case for which the minimum of such curves does not have a horizontal tangent. This is due to the fact that the denominator in $\mathcal{D}'$ annihilates as well as the numerator. Moreover, this is the limiting situation when the "pockets" of asymptotic stability present for $a_{0,R} < 1$ (Figure 7) disappear (Figure 8). Finally, as far as $a_{0,R} = \frac{\pi}{2}$, the minimum point coincide with the lowest intersections of the oblique asymptotes.

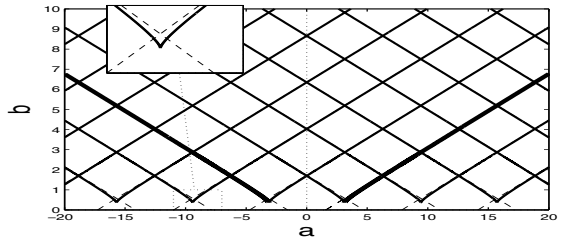

Figure 10. Imaginary crossings for $a_{0,R} = 1$.

So far in this Section we devoted our attention to recover the regions of asymptotic stability for (3), or better, all the curves corresponding to roots crossing the imaginary axis for (3) or the vertical axis $\gamma = -a_{0,R}$ for (5). As a final target, we now investigate the exactness of our findings on the location of the characteristic roots of (3). This is done simply by comparing the intersection $\mathcal{E} \cap \mathcal{T}$ relevant to (5) and shifted back through (18), with accurate approximations computed via the numerical method in Breda et al. (2005). A single example is given in Figure 12 (other choices of a_0, b_0 lead to similar results).

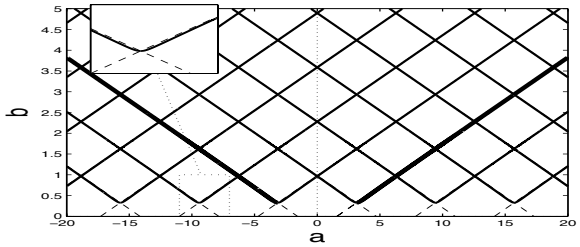

Figure 11. Imaginary crossings for $a_{0,R} = \frac{\pi}{2}$.

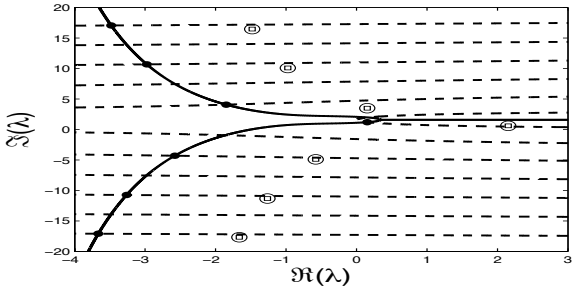

Figure 12. $a_0 = 2 + \mathrm{i}$ and $b_0 = 3 - 2\mathrm{i}$: roots of (5) from $\mathcal{E} \cap \mathcal{T}$ (•), roots of (3) by shift (□), by numerics (○).

REFERENCES

Bozzo, E., Breda, D., and Vermiglio, R. (2010). A survey on roots and charts of delay differential equations. In preparation.

Breda, D., Maset, S., and Vermiglio, R. (2005). Pseudospectral differencing methods for characteristic roots of delay differential equations. *SIAM J. Sci. Comput.*, 27(2), 482–495.

Butcher, E.A., Ma, H.T., Bueler, E., Averina, V., and Szabo, Z. (2004). Stability of linear time-periodic delay-differential equations via chebyshev polynomials. *Int. J. Numer. Meth. Engng*, 59, 895–922.

Engelborghs, K. and Roose, D. (2002). On stability of LMS methods and characteristic roots of delay differential equations. *SIAM J. Numer. Anal.*, 40(2), 629–650.

Hale, J.K. (1977). *Introduction to functional differential equations.* Number 99 in AMS series. Springer Verlag, New York, USA, 1st edition.

Jarlebring, E. (2008). *The spectrum of delay-differential equations: numerical methods, stability and perturbation.* Ph.D. thesis, Inst. Comp. Math, TU Braunschweig.

Jarlebring, E. and Damm, T. (2007). The Lambert W function and the spectrum of some multidimensional time-delay systems. *Automatica*, 43(12), 2124–2128.

Maset, S. (2000). Stability of Runge-Kutta methods for linear delay differential equations. *Numer. Math.*, 87, 355–371.

Radjavi, H. and Rosenthal, P. (2000). *Simultaneous Triangularization.* Universitext. Springer, New York, USA.

Sipahi, R., Gürdal, A., and Niculescu, S.I. (2006). Characterization of the stability of gradient play games with time delayed derivative approximation actions. In *Control and Decision Conference (CDC 2006).*

Vyhlídal, T. and Zítek, P. (2006). Mapping the spectrum of a retarded time-delay system utilizing root distribution features. In C. Manes and P. Pepe (eds.), *Time Delay Systems*, volume 6. Elsevier.